

Analytical Calculations of the Stark Broadening of Hydrogen/ Deuterium Spectral Lines by a Relativistic Electron Beam: Applications to Magnetic Fusion Edge Plasmas

E. OKS*Physics Department, 206 Allison Lab, Auburn University, Auburn, AL 36849, USA*

ABSTRACT: Theory of the Stark broadening of hydrogen/deuterium spectral lines by a Relativistic Electron Beam (REB) is presented. The theory is developed analytically by using an advanced formalism. Possible applications of these analytical results to magnetic fusion edge plasmas are discussed.

Key words: Stark broadening, hydrogen/deuterium spectral lines, relativistic electron beam, magnetic fusion

1. INTRODUCTION

The interaction of a Relativistic Electron Beam (REB) with plasmas has both the fundamental importance for understanding physics of plasmas and practical applications. The latter include (but not limited to) plasma heating, inertial fusion, generation of high-intensity coherent microwave radiation, acceleration of charged particles in plasmas – see, e.g., papers [1-3] and references therein.

The latest (though negative) application relates to magnetic fusion and deals with runaway electrons. In some discharges in tokamaks, the plasma current decays and is partly replaced by runaway electrons that reach relativistic energies: this poses danger to the mission of the next generation tokamak ITER – see, e.g., papers [4-6] and references therein. At various discharges at different tokamaks, such as, e.g., those presented in papers [7-9], the energy of the runaway electrons was measured in the range $\sim (0.2 - 10)$ MeV and the ratio of their density to the density of the bulk plasma electrons was measured in the range $\sim (10^{-1} - 10^{-4})$.

Therefore developing diagnostics of a REB and its interaction with plasmas should be important. In the particular case of tokamaks, the development of a REB should be timely detected to allow the mitigation of the problem.

Diagnostics based on the analysis of spectral line shapes have known advantages over others. They are not intrusive and allow measuring plasma parameters and parameters of various fields in plasmas without perturbing the parameters to be measured – see, e.g., books [10-15].

In the current paper we present a theory of the Stark broadening of hydrogen/deuterium spectral lines by a REB. The theory is developed analytically by using an advanced formalism. We discuss possible applications of these analytical results to magnetic fusion edge plasmas*.

* We note that Rosato et al [16] attempted studying the Stark broadening of hydrogen line by a REB in magnetic fusion edge plasmas. However, they used the quasistatic approximation, which is totally inappropriate for the broadening by fast electrons of a REB (it is inappropriate even for the broadening by thermal electrons in such plasmas).

2. ANALYTICAL RESULTS AND APPLICATIONS TO MAGNETIC FUSION

The presence of a REB introduces anisotropy in the process of the Stark broadening of spectral lines in plasmas. A different kind of anisotropic Stark broadening was first considered by Seidel in 1979 [17] for the following situation. If hydrogen atoms radiate from a plasma consisting mostly of much heavier ions, then in the reference frame moving with the velocity v of the radiating hydrogen atom, the latter “perceives” a beam of the much heavier ions moving with the velocity v . Seidel [17] treated this situation by applying the so-called standard (or conventional) theory of the impact broadening of hydrogen lines, also known as Griem’s theory [18]. Therefore, while Seidel [17] should be given credit for pioneering the anisotropic Stark broadening, his specific calculations had a weakness that plagues the standard theory: the inherent divergence at small impact parameters causing the need for a cutoff defined only by an order of magnitude.

Later in paper [19] the authors considered the same situation as Seidel [17], but applied a more advanced theory of the Stark broadening called the generalized theory developed in paper [20] and presented also in book [12]. (It should be emphasized that in paper [19] it was the application of the “core” generalized theory from paper [20] without the additional effects that were introduced later and were the subject of discussions in the literature.) The authors of paper [19] took into the exact account (in all the orders of the Dyson expansion) the projection of the dynamic, heavy-ion-produced electric field onto the velocity of the radiator exactly. As a result, there was no divergence at small impact parameters and thus no need for the imprecise cutoff.

In the present paper we use the formalism from paper [19] to treat the Stark broadening of hydrogen/deuterium spectral lines by a REB in plasmas. There are two major distinctions from paper [19]: 1) the broadening is by a beam of electrons rather than ions; 2) the electrons are relativistic.

Following paper [19] we choose the z -axis in the direction of the REB and represent the Hamiltonian $H(t)$ perturbed by the field $\mathbf{E}(t)$ of the REB in the form:

$$H(t) = H_1(t) + V(t), \quad H_1(t) \equiv H_0 - d_z E_z(t), \quad V(t) \equiv -d_x E_x - d_y E_y. \quad (1)$$

The partial time-dependent Hamiltonian $H_1(t)$ is diagonalized here in the parabolic quantization and is allowed for exactly. The residual interaction $V(t)$ is taken into account via the Dyson perturbation expansion.

The starting expression for the lineshape $I(\omega, \nu)$ depends on the velocity ν of the REB:

$$I(\omega, \nu) = -\frac{1}{\pi} \operatorname{Re} \sum_{\sigma} \sum_{\alpha\alpha'\beta\beta'} \langle \beta | d_{\sigma} | \alpha \rangle \langle \alpha' | d_{\sigma} | \beta' \rangle \langle \langle \alpha\beta | G^{-1} | \alpha' \beta' \rangle \rangle. \quad (2)$$

Here α, α' and β, β' label the Stark sublevels of the upper (a) and lower (b) states involved in the radiative transition; d_{σ} are components of the dipole moment operator; the spectral operator G is

$$G = i\Delta\omega + \Phi_{ab}(\nu), \quad (3)$$

where the impact operator $\Phi_{ab}(\nu)$ is

$$\Phi_{ab} = N_b \nu \int_0^{\infty} 2\pi\rho \, d\rho \{ S_a S_b^* - I \}_{\bar{\rho}}. \quad (4)$$

Here N_b is the electron density of the REB.

The operator $\Phi_{ab}(\nu)$ is subdivided into adiabatic $\Phi_{ab}^{\text{ad}}(\nu)$ and nonadiabatic $\Phi_{ab}^{\text{na}}(\nu)$ contributions

$$\Phi_{ab}(\nu) = \Phi_{ab}^{\text{ad}}(\nu) + \Phi_{ab}^{\text{na}}(\nu), \quad (5)$$

where $\Phi_{ab}^{\text{ad}}(\nu)$ contains only the following combination of the diagonal matrix elements of the dipole moment operator: $e^2(z_{\alpha\alpha} - z_{\beta\beta})^2$. An important feature of the impact Stark broadening by a beam of ions or electrons is that the

adiabatic part $\Phi_{ab}^{ad}(\nu)$ vanishes - in distinction to the impact Stark broadening by randomly moving thermal ions or electrons [19].

The scattering matrix S entering Eq. (4) is represented in the form:

$$S = \exp\left[(i/\hbar) \int_{-\infty}^{\infty} dt d_z E_z(t)\right] \hat{T} \exp\left[(i/\hbar) \int_{-\infty}^{\infty} dt Q^* (d_x E_x + d_y E_y) Q\right],$$

$$Q = \exp\left[-(i/\hbar) \left(H_0 t - \int_{-\infty}^t dt' d_z E_z(t')\right)\right]. \quad (6)$$

For Lyman lines the scattering matrix $S_b=1$, what simplifies calculations. Then in the second order of the modified Dyson expansion (6), the matrix elements of the nonadiabatic part of the operator $\Phi_{ab}(\nu)$ are:

$$\Phi_{\alpha\alpha'} = -4\pi N_b \frac{e^2}{\hbar^2 v} \sum_{\alpha''} d_{\alpha\alpha''}^x d_{\alpha''\alpha'}^x \int_0^{\infty} C_{\pm}(Z) \frac{dZ}{Z}. \quad (7)$$

Here

$$Z = 2m_e v\rho/(3n\hbar), \quad (8)$$

where n is the principal quantum number of the upper level and ρ is the impact parameter. So, physically the quantity Z is the scaled, dimensionless impact parameter and the integration over Z in Eq. (7) corresponds to the integration over impact parameters.

If the electron beam would be a non-relativistic, so that the electric field produced by the beam electron at the location of the radiating atom would be

$$\mathbf{E}(t) = e\mathbf{r}(t)/r^3(t), \quad (9)$$

where $\mathbf{r}(t)$ is the radius vector from the beam electron to the radiating atom, then the broadening functions C_+ and C_- entering Eq. (7) for nondiagonal and for diagonal matrix elements, respectively, would be the following double integrals:

$$C_{\pm}(Z) = \frac{1}{2} \int_{-\infty}^{\infty} \int_{-\infty}^{x_1} \frac{dx_1 dx_2}{[g(x_1)g(x_2)]^3} \exp\left[\frac{i}{Z} (1/g(x_1) \pm 1/g(x_2))\right],$$

$$g(x) \equiv \sqrt{1 + x^2}. \quad (10)$$

However, for the REB, Eq. (9) has to be modified to (see, e.g., Eq. (38.8) from book [21]):

$$\mathbf{E}(t) = e\mathbf{r}(t) / [r^3(t)\gamma^2(\cos^2\theta + \sin^2\theta/\gamma^2)^{3/2}]. \quad (11)$$

Here

$$\gamma = 1/(1 - v^2/c^2)^{1/2} \quad (12)$$

is the relativistic factor and $\theta(t)$ is the angle between the beam velocity \mathbf{v} and vector $\mathbf{r}(t)$, so that

$$\cos^2\theta = v^2 t^2/(\rho^2 + v^2 t^2), \quad \sin^2\theta = \rho^2/(\rho^2 + v^2 t^2), \quad (13)$$

the instant $t = 0$ corresponding to the closest approach of the beam electron to the radiating atom.

The relativistic counterparts C_{r+} and C_{r-} of the broadening functions C_+ and C_- become as follows:

$$C_{r\pm}(Z) = \frac{I}{2\gamma^4} \int_{-\infty}^{\infty} \int_{-\infty}^{x_1} \frac{dx_1 dx_2}{[g_r(x_1)g_r(x_2)]^3} \exp\left[\frac{i}{Z}(I/g_r(x_1) \pm I/g_r(x_2))\right], \quad (14)$$

$$g_r(x) \equiv \sqrt{I/\gamma^2 + x^2}.$$

For the real parts $A_{r\pm} = \text{Re } C_{r\pm}$, the double integral in Eq. (14) can be calculated analytically. It yields:

$$A_{r-} = (\pi/2)^2 [\mathbf{H}_{-1}(1/s) + J_1(1/s)], \quad A_{r+} = (\pi/2)^2 [\mathbf{H}_{-1}(1/s) - J_1(1/s)], \quad s = Z/\gamma, \quad (15)$$

where $\mathbf{H}_{-1}(1/s)$ and $J_1(1/s)$ are Struve and Bessel functions, respectively. Below we omit the suffix “r” for brevity.

The width of spectral line components is controlled by the subsequent integral over the scaled impact parameter Z :

$$a_{\pm} = \int_0^{Z_{\max}} A_{\pm}(Z) dZ/Z = \int_0^{Z_{\max}/\gamma} A_{\pm}(s) ds/s, \quad s = Z/\gamma. \quad (16)$$

Figure 1 shows the plot of the integrand $A_{-}(s)/s$ versus s . It is seen that the corresponding integral a_{-} does not diverge at small impact parameters.

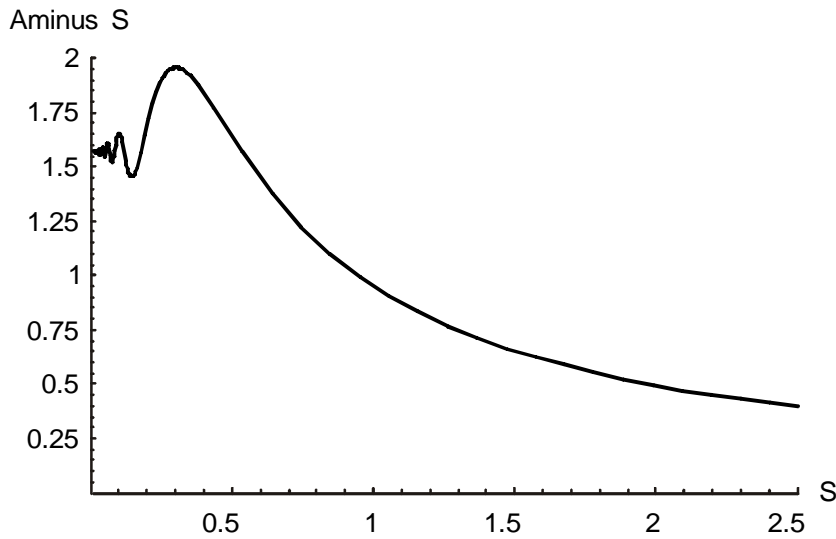


Figure 1: The integrand $A_{-}(s)/s$, corresponding to the widths function a_{-} , versus $s = Z/\gamma$, where Z is the scaled impact parameter defined by Eq. (8) and γ is the relativistic factor defined by Eq. (12)

Figure 2 presents the plot of the integrand $A_{+}(s)/s$ versus s and Fig. 3 shows a magnified part of this plot at small impact parameters. It is seen that the corresponding integral a_{+} also does not diverge at small impact parameters.

Thus, the integrals over the scale impact parameter Z in Eq. (16) converge at small impact parameters – in distinction to what would have resulted from the standard theory. At large Z the integral diverge (just as what would have resulted from the standard theory), which is physically because of the long-range nature of the Coulomb interaction between the charged particles. However, due to the Debye screening in plasmas, there is a natural upper cutoff Z_{\max} :

$$Z_{\max} = uZ_0, \quad u = v/c = (1 - 1/\gamma^2)^{1/2}, \quad Z_0 = 2m_e c \rho_D / (3n\hbar). \quad (17)$$

Here

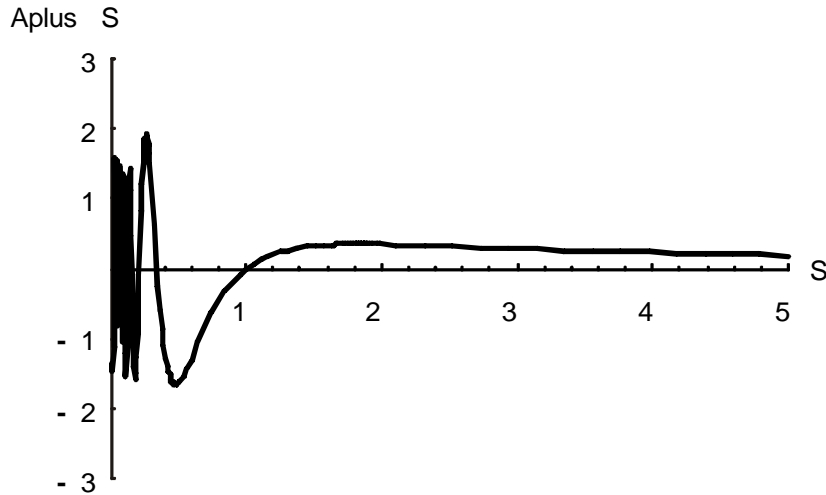


Figure 2: The integrand $A_+(s)/s$, corresponding to the widths function a_+ , versus $s = Z/\gamma$, where Z is the scaled impact parameter defined by Eq. (8) and γ is the relativistic factor defined by Eq. (12)

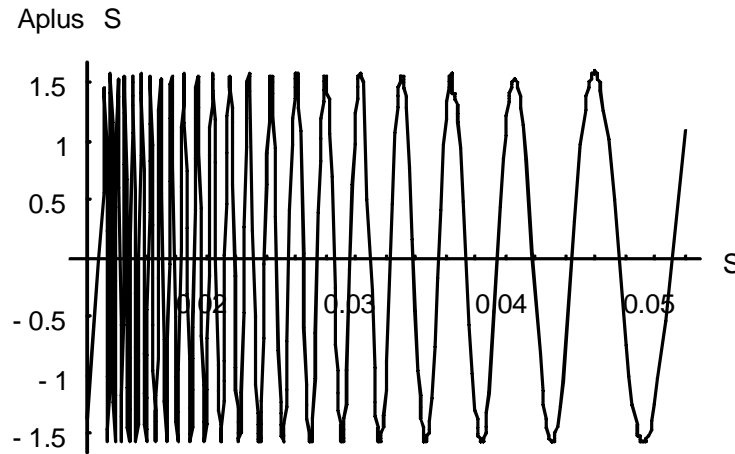


Figure 3: Same as in Fig. 2, but for small impact parameters

$$\rho_D = [T_e / (4\pi e^2 N_e)]^{1/2} \quad (18)$$

is the Debye radius; T_e and N_e are the temperature and the density of bulk electrons, respectively.

The integration in Eq. (16) can be performed analytically because the integrals in Eq. (16) have the following antiderivatives

$$j_{\pm}(s) = \int A_{\pm}(s) ds/s = (\pi^2/8) \{ (2/\pi) \text{MeijerG}[\{\{0\}, \{1\}\}, \{\{0,0\}, \{-1/2, 1/2\}\}, 1/(4s^2)] + \quad (19)$$

$$\mathbf{H}_{-1}^2(1/s) + \mathbf{H}_0^2(1/s) \pm [1 - {}_1F_2(1/2; 1, 2; -1/s^2)],$$

where Meijer $G[\dots]$ and ${}_1F_2(\dots)$ are the MeijerG function and the generalized hypergeometric function, respectively. Thus, we obtain analytical results for the width functions:

$$a_{\pm} = j_{\pm}(Z_{\max}/\gamma) - j_{\pm}(0). \quad (20)$$

Below, as an example, we calculate explicitly the shape $I(\Delta\omega, \gamma)$ of the spectral line Ly-alpha broadened by a REB, where $\Delta\omega$ is the detuning from the unperturbed frequency of the spectral line. Similarly to paper [19], after inverting of the spectral operator, we obtain:

$$I(\Delta\omega, \gamma) = \frac{1}{3\pi} \left(\frac{\Gamma_\pi}{\Delta\omega^2 + \Gamma_\pi^2} + \frac{2\Gamma_\sigma}{\Delta\omega^2 + \Gamma_\sigma^2} \right), \quad (21)$$

where Γ_π and Γ_σ are the half-widths at half-maximum of the π - and σ -components of the Ly-alpha line, respectively. They are expressed as follows:

$$\Gamma_\sigma = [\eta_0 / (1 - 1/\gamma^2)^{1/2}] [j_-(Z_{\max} / \gamma) - j_-(0)], \quad (22)$$

$$\Gamma_\pi = [\eta_0 / (1 - 1/\gamma^2)^{1/2}] \int_0^\infty [A_-(s) - A_+(s)] ds / s, \quad (23)$$

where

$$\eta_0 = 4\pi\hbar^2 N_e / (m_e^2 c) = 5.618 \times 10^{10} N_e (\text{cm}^{-3}) s^{-1}. \quad (24)$$

It is worth noting that in Eq. (23), the upper limit of the integration is infinity. This is because for the π -component of the Ly-alpha line the width in Eq. (23) is proportional to the difference of diagonal and nondiagonal matrix elements of the broadening operator, so that the corresponding integral converges not only at small, but also at large impact parameters, yielding the following relatively simple expression for the width:

$$\Gamma_\pi = \pi^2 \eta_0 / [4(1 - 1/\gamma^2)^{1/2}]. \quad (25)$$

Figure 4 shows the plot of the scaled width of the σ -component Γ_σ / η_0 (upper curve) and of the scaled width of the π -component Γ_π / η_0 (lower curve) of the Ly-alpha line broadened by a REB versus the relativistic factor γ at $N_e = 10^{15} \text{ cm}^{-3}$ and $T_e = 2 \text{ eV}$. It is seen that as γ increases from unity, both widths significantly decrease.

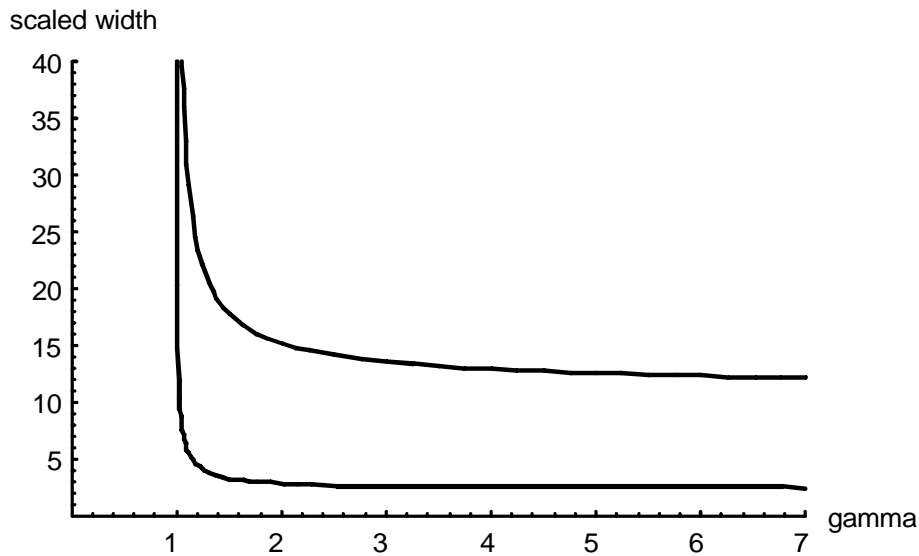


Figure 4: The scaled width of the σ -component Γ_σ / η_0 (upper curve) and the scaled width of the π -component Γ_π / η_0 (lower curve) of the Ly-alpha line broadened by a REB versus the relativistic factor γ at $N_e = 10^{15} \text{ cm}^{-3}$ and $T_e = 2 \text{ eV}$

Figure 5 presents the ratio $\Gamma_\sigma / \Gamma_\pi$ versus the relativistic factor γ at $N_e = 10^{15} \text{ cm}^{-3}$ and $T_e = 2 \text{ eV}$. It is seen that as γ increases from unity, this ratio increases, then reaches the maximum, and then decreases. The maximum ratio $\Gamma_\sigma / \Gamma_\pi = 5.39$ corresponds to $\gamma = 2^{1/2}$.

Separate measurements of the widths of the σ - and π -components (and thus of the ratio $\Gamma_\sigma / \Gamma_\pi$) can be performed for the observation perpendicular to the REB velocity by placing a polarizer into the optical system: when the axis

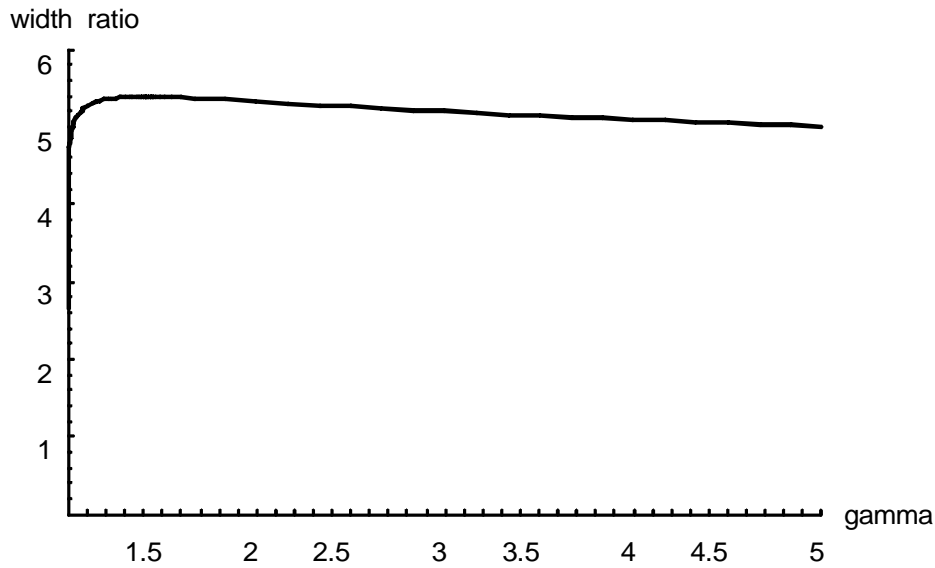


Figure 5: Ratio $\Gamma_\sigma / \Gamma_\pi$ of the widths of the σ - and π -components of the Ly-alpha line versus the relativistic factor γ at $N_e = 10^{15} \text{ cm}^{-3}$ and $T_e = 2 \text{ eV}$

of the polarizer would be perpendicular or parallel to the REB velocity, then one would be able to measure Γ_σ or Γ_π , respectively. By monitoring the dynamics of the ratio $\Gamma_\sigma / \Gamma_\pi$, it would be possible, at least in principle, to detect the development of a REB in tokamaks and to engage the mitigation of the problem.

Figure 6 shows the theoretical profiles of the entire Ly-alpha line, corresponding to the observation perpendicular to the REB velocity without the polarizer, at $N_e = 10^{15} \text{ cm}^{-3}$ and $T_e = 2 \text{ eV}$. The profiles were calculated using Eqs. (21) – (24) and presented versus the scaled detuning $\Delta\omega / \Gamma_\pi$ denoted as d . Due to the scaled detuning, the profiles are “universal” in the sense that they are independent of the beam electron density. The solid curve corresponds to $\gamma = 2^{1/2}$, while the dashed curve – to $\gamma = 1$. In the case of $\gamma = 2^{1/2}$, the profile is by 12% narrower than for the case of

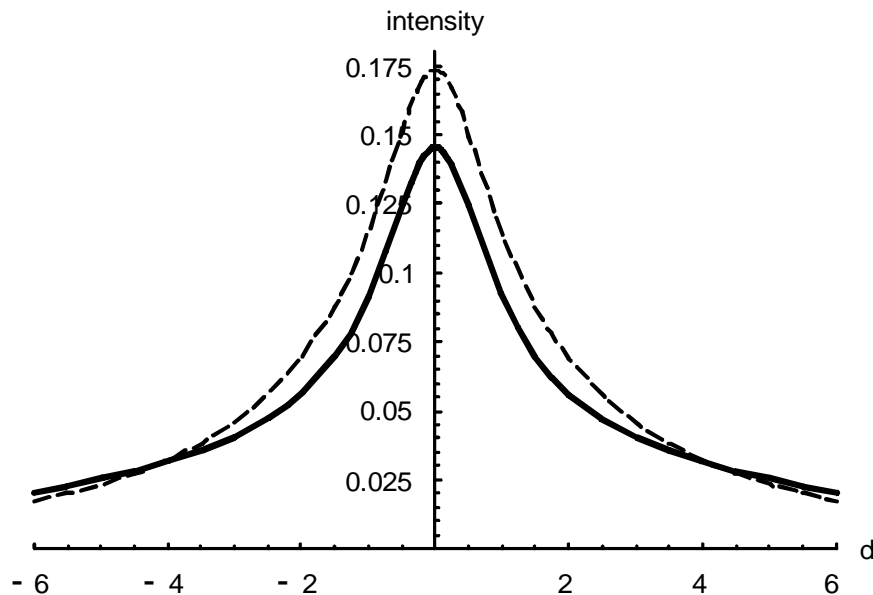


Figure 6: Theoretical profiles of the entire Ly-alpha line, corresponding to the observation perpendicular to the REB velocity without the polarizer, at $N_e = 10^{15} \text{ cm}^{-3}$ and $T_e = 2 \text{ eV}$. The profiles were calculated using Eqs. (21) – (24) and presented versus the scaled detuning $\Gamma\omega / \Gamma_\pi$ denoted as d . The solid curve corresponds to $\gamma = 2^{1/2}$, while the dashed curve – to $\gamma = 1$

$\gamma = 1$. Detecting the development of a REB via such relatively small decrease of the width seems to be less advantageous compared to the polarization analysis of the width discussed above, where the widths ratio Γ_σ/Γ_π could increase by an order of magnitude as a REB develops in the plasma.

The above theoretical results represented the Stark broadening of hydrogen/deuterium spectral lines only by a REB without allowing for other factors affecting the lineshapes. This was done for presenting the effect of a REB on the lineshape in the “purest” form*.

3. CONCLUSIONS

We developed an advanced analytical theory of the Stark broadening of hydrogen/deuterium spectral lines by a REB. We showed that the final stage of the development of the REB (where the beam electron density N_b could become just of one or two orders of magnitude below the electron density N_e of bulk electrons), would be manifested – and thus could be detected, at least in principle – by a decrease of the width of hydrogen/deuterium spectral lines. We demonstrated that especially sensitive to the final stage of the development of the REB would be the ratio of widths of σ - and π -components, which could be determined by the polarization analysis.

References

- [1] D. Guenot, D. Gustas, A. Vernier, B. Beaufrepaire, F. Böhle, M. Bocoum, M. Losano, A. Jullien, A. Lopez-Martins, A. Lifschitz, and J. Faure, *Nature Photonics* **11** (2017) 293.
- [2] S. A. Kurkin, A.E. Hramov, and A. A. Koronovskii, *Appl. Phys. Letters* **103** (2013) 043507.
- [3] P. C. de Jagher, F.W. Sluijter, and H. J. Hopman, *Phys. Reports* **167** (1988) 177.
- [4] A. H. Boozer, *Nuclear Fusion* **57** (2017) 056018.
- [5] J. Decker, E. Hirvijoki, O. Embreus, Y. Peysson, A. Stahl, I. Pusztai, and T. Fülöp, *Plasma Physics and Controlled Fusion* **58** (2016) 025016.
- [6] H. Smith, P. Helander, L.-G. Eriksson, D. Anderson, M. Lisak, and F. Andersson, *Physics of Plasmas* **13** (2006) 102502.
- [7] P.V. Minashin, A.B. Kukushkin, and V.I. Poznyak, *EPJ Web of Conferences* **32** (2012) 01015.
- [8] B. Kurzan, K.-H. Steuer, and W. Suttrop, *Rev. Sci. Instrum.* **68** (1997) 423.
- [9] S. Ide, K. Ogura, H. Tanaka, M. Iida, K. Hanada, T. Itoh, M. Iwamasa, H. Sakakibara, T. Minami, M. Yoshida, T. Maekawa, Y. Terumichi, and S. Tanaka, *Nuclear Fusion* **29** (1989) 1325.
- [10] E. Oks, *Diagnostics of Laboratory and Astrophysical Plasmas Using Spectral Lines of One-, Two-, and Three-Electron Systems* (World Scientific, New Jersey) 2017.
- [11] H.-J. Kunze, *Introduction to Plasma Spectroscopy* (Springer, Berlin) 2009.
- [12] E. Oks, *Stark Broadening of Hydrogen and Hydrogenlike Spectral Lines in Plasmas: The Physical Insight* (Alpha Science International, Oxford, UK) 2006.
- [13] T. Fujimoto, *Plasma Spectroscopy* (Clarendon Press, Oxford, UK) 2004.
- [14] H. R. Griem, *Principles of Plasma Spectroscopy* (Cambridge University Press, Cambridge) 1997.
- [15] E. Oks, *Plasma Spectroscopy: The Influence of Microwave and Laser Fields*, Springer Series on Atoms and Plasmas, vol. 9 (Springer, New York) 1995.
- [16] J. Rosato, S. P. Pandya, Ch. Logeais, M. Meireni, I. Hannachi, R. Reichle, R. Barnsley, Y. Marandet, and R. Stamm, *AIP Conf. Proceedings* **1811** (2017) 110001.
- [17] J. Seidel, *Z. Naturforsch.* **34a** (1979) 1385.

* So far we used, as an example the Ly-alpha line just to get the message across (since we obtained relatively simple analytical expressions for the shape of this line). We note that at $N_e \sim 10^{15} \text{ cm}^{-3}$, the Stark width of the Lyman-alpha line calculated by Eqs. (22) – (25) would be by about two and a half orders of magnitude below the natural width. However, the dynamical Stark width scales $\sim n^4$, while the natural width scales $\sim 1/n^3$ (n being the principal quantum number). Therefore, for the lines originating from the level of $n = 4$ (such as Ly-gamma, Balmer-beta, Paschen-alpha) and higher levels, the corresponding dynamical Stark width would exceed the natural width.

- [18] H.R. Griem, *Spectral Line Broadening by Plasmas* (Academic, New York) 1974.
- [19] A. Derevianko and E. Oks, *J. Quant. Spectrosc. Rad. Transfer* **54** (1995) 137.
- [20] Ya. Ispolatov and E. Oks, *J. Quant. Spectrosc. Rad. Transfer* **51** (1994) 129.
- [21] L.D. Landau and E.M. Lifshitz, *The Classical Theory of Fields* (Pergamon, Oxford) 1971.